

Unsteady discharge calibration of a large V-notch weir

Hubert Chanson*, Hang Wang

The University of Queensland, School of Civil Engineering, Brisbane, QLD 4072, Australia

ARTICLE INFO

Article history:

Received 13 July 2012

Received in revised form

16 October 2012

Accepted 16 October 2012

Available online 29 October 2012

Keywords:

90° V-notch weir

Unsteady experiments

Calibration

Discharge measurement

Seiche

Sloshing

Dam break wave

Physical modelling

Triangular V-notch thin-plate weir

ABSTRACT

Thin-plate weirs are commonly used as measuring devices in flumes and channels, enabling an accurate discharge measurement with simple instruments. The calibration formulae of such devices rely upon some empirical coefficients and there is a need to obtain new accurate physical data to complement the existing evidence. In the present study, the discharge calibration of a large 90° V-notch thin plate weir was performed using an unsteady volume per time technique. The V-notch weir was initially closed by a fast-opening gate. The sudden opening induced an initial phase of the water motion dominated by the free-falling motion of a volume of fluid in the vicinity of the weir, followed by a gradually-varied phase, during which some seiche was observed in the tank. The relationship between water discharge and upstream water elevation was derived from the integral form of the continuity equation. The results yielded a dimensionless discharge coefficient $C_d = 0.58$ close to previous experiments for 90° V-notch weirs. The findings showed that the unsteady discharge calibration of the V-notch weir yielded similar results to a more traditional calibration approach based upon steady flow experiments, allowing a rapid testing over a broad range of flow rates.

© 2012 Elsevier Ltd. All rights reserved.

1. Introduction

In open channel flows, the knowledge of the water discharge is a key parameter, and a range of measurement techniques were developed [4,8,10]. Many techniques rely upon some empirical coefficients [1] and there is a need to obtain new accurate physical data to complement the existing evidence. Flow measuring structures in waterworks, canals and wastewater plants consist mainly of flumes and thin plate weirs [5,9]. Thin-plate weirs enable an accurate discharge measurement with simple instruments [16]. The V-notch weirs, also called triangular weirs, have an overflow edge in the form of an isosceles triangle. Fig. 1 presents a sketch of a 90° V-notch weir. Ref. [3] expresses the discharge calibration of a triangular V-notch thin-plate weir in the form:

$$Q = C_d \times \frac{8}{15} \times \tan \alpha \times \sqrt{2 \times g \times h^5} \quad (1)$$

where Q is the water discharge, C_d a dimensionless discharge coefficient, α the notch opening angle, g the gravity acceleration and h the upstream water elevation above the notch (Fig. 1). Basic dimensional considerations show that the discharge coefficient C_d is a function of the notch angle α , the relative weir height p/W and relative upstream depth h/p (Fig. 1). Ref. [13] presented some seminal experiments conducted with five different fluids (Table 1),

while Refs. [5] and [9] reviewed recent findings based upon steady flow experiments.

A very robust discharge measurement technique is the volume per time method: “the only rational method of calibrating weirs, i.e. in accordance with hydrometric principles, is the volumetric method, which depends on measuring the volume, with a measuring reservoir, and the time of flow” ([16], p. 310). The technique may be adapted to unsteady flow situations (e.g., [6,15]). The contribution herein presents a novel approach to determine the discharge calibration of a large 90° V-notch weir and associated accuracy based upon a comprehensive physical study. The calibration was undertaken using a volume per time approach by measuring the upstream water level at high frequency following a sudden gate opening. The results showed the application of the technique and highlighted a number of practical issues. The paper is complemented by a digital appendix with two movies (Table 2).

Supplementary material related to this article can be found online at <http://dx.doi.org/10.1016/j.flowmeasinst.2012.10.010>.

2. Materials and methods

2.1. Experimental facility and instrumentation

The experiments were performed with a 400 mm high 90° V-notch thin-plate weir. The weir was installed at one end of a 2.36 m long, 1.66 m wide and 1.22 m deep tank (Figs. 2 and 3, Table 1). The bottom of the V-notch was located 0.82 m above the

* Corresponding author. Tel.: +61 7 3365 3619; fax: +61 7 3365 4599.

E-mail address: h.chanson@uq.edu.au (H. Chanson).

URL: <http://www.uq.edu.au/~e2hchans/> (H. Chanson).

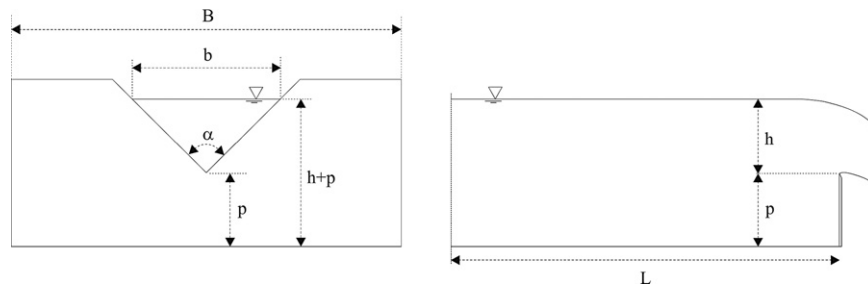


Fig. 1. Sketch of a triangular V-notch thin-plate weir.

Table 1
Experimental studies of 90° V-notch weirs.

Ref. [1]	Fluid(s) (2)	<i>h</i> (m) (3)	<i>p</i> (m) (4)	<i>B</i> (m) (5)	Fluid properties (7)	Remarks (7)
[13]	Water	0.070–0.152	0.91	1.07	<i>s</i> = 1	Tests at the University of Wisconsin
	Fuel oil (Oil A)	0.018–0.122			<i>s</i> = 0.90–0.91 <i>v</i> = 0.5 to 1.5 × 10 ^{−4} m ² /s <i>σ</i> = 0.03–0.031 N/m	
	Dustproofing oil (Oil G)	0.046–0.122			<i>s</i> = 0.89–0.91 <i>v</i> = 0.12 to 0.5 × 10 ^{−4} m ² /s <i>σ</i> = 0.03–0.032 N/m	
	Oil C	0.03–0.055	–	0.263	<i>s</i> = 0.87–0.88 <i>v</i> = 0.25 to 0.7 × 10 ^{−4} m ² /s <i>σ</i> = 0.033 N/m	Tests at the University of California, Berkeley
	Oil M	0.037 to 0.061			<i>s</i> = 0.85–0.86 <i>v</i> = 0.07 to 0.2 × 10 ^{−4} m ² /s <i>σ</i> = 0.032 N/m	
	Water	0.046–0.67	2.44	1.83	<i>s</i> = 1	Tests at the Cornell University
Present study	Water	0.40	0.82	1.66	<i>s</i> = 1 Water temperature: 16.5 °C <i>ρ</i> = 998.8 kg/m ³ <i>v</i> = 1.10 × 10 ^{−6} m ² /s <i>σ</i> = 0.0739 N/m	Unsteady tests. <i>L</i> = 2.36 m. <i>B</i> = 1.66 m.

Notes: *h*: upstream water elevation above notch; *s*: relative density; *ρ*: density; *v*: kinematic viscosity; *σ*: surface tension.

tank invert. The V-notch was made out of brass and designed based upon Ref. [3] (also [11]). The notch was initially closed with a fast-opening gate hinging outwards and upwards (Table 2).

During static tests, the water depths were measured using a pointer gauge. For the dynamic tests, the unsteady water depth was measured using a series of three acoustic displacement meters Microsonic™ Mic+25/IU/TC located 1.11 m upstream of the weir (Fig. 3). The displacement sensors had a range of 220 mm, and they were positioned at various elevations to cover the full range of free-surface elevations (i.e. 400 mm). The data accuracy and response time of the acoustic displacement meters were 0.18 mm and 50 ms respectively. All the displacement sensors were synchronised and sampled simultaneously at 200 Hz.

Additional visual observations were recorded with two HD digital video cameras, two dSLR cameras Pentax™ K-01 and K-7, and a Pentax™ Optio WG-01 digital camera. The dSLR cameras Pentax™ K-01 and K-7 were equipped with Pentax™ DA40 mm f2.8 XS and Pentax™ SMC FA31 mm f1.8 Limited prime lenses respectively, exhibiting only slight barrel distortions: that is, about 0.6% and 0.8% respectively. Some coloured vegetable dye was added to the water to improve the visibility of the streamlines (e.g. Fig. 3). Further details of the experiments were reported in [7].

2.2. Experimental flow conditions

The displacement meters were located 1.11 m upstream of the weir about the tank centreline (Fig. 3). The video-cameras were placed around the tank at various locations to cover both the water motion in the tank and weir overflow during each test.

For each experimental run, the tank was filled slowly to the brink of the brass plate. The tests were conducted with the reservoir initially full: i.e., *h*₀ = 0.4 m where *h*₀ is the initially steady water level above the lower edge of the notch. The water was left to settle for several minutes prior to start. The experiment started when the gate was opened rapidly and the water level was recorded continuously for 500 s. The gate was operated manually and the opening times were less than 0.15–0.2 s. Such an opening time was small enough to have a negligible effect on the water motion in the tank [12]. After the rapid gate opening, the gate did not intrude into the flow as seen in the photographs and movies (Table 2).

3. Results

The water level in the tank was initially still prior to gate opening. The water level fluctuations recorded by the sensors were within the accuracy of the sensor: *h*₀' ≈ 0.17 mm on average where *h*₀' is the standard deviation of the initially steady water level above the lower edge of the notch. The gate opening was rapid and lasted less than 0.2 s. Figs. 2 and 3 illustrate some typical gate opening sequence. The unsteady flow above the weir consisted of an initial phase dominated by the free-falling motion of a volume of fluid in the vicinity of the notch, followed by a gradually-varied flow motion. The manuscript is supplemented by two video movies: IMGPO123.mpg and IMGPO571.mpg (Table 2). The movie IMGPO123.mpg shows the side view of sudden gate during Run 2 (Duration: 8 s). The movie IMGPO571.mpg presents a view from upstream of the tank and sudden gate opening during Run 5 (Duration: 12 s).



Fig. 2. Side view photographs of the gate opening—experimental run no. 2, $h_o = 0.40$ m, camera: Pentax K-7, lens: Pentax FA31 mm f1.8 Limited, shutter 1/80s—from left to right, top to bottom: $t = 0, 0.19$ s, 0.38 s and 0.58 s.

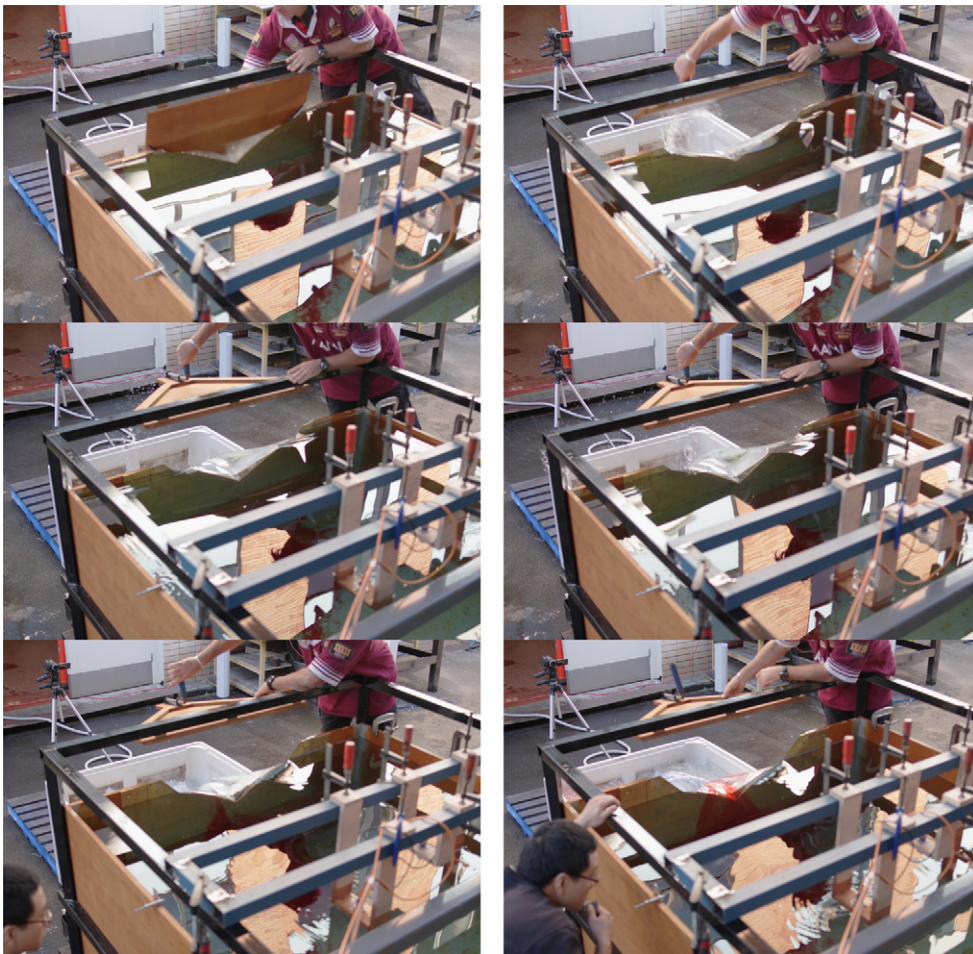


Fig. 3. General view of the reservoir and V-notch weir during the gate opening— $h_o = 0.40$ m—camera: Pentax K-7, lens: Pentax FA31 mm f1.8 Limited, shutter 1/125s—from left to right, top to bottom: $t = T_o, T_o + 0.19$ s, $T_o + 0.38$ s, $T_o + 0.58$ s, $T_o + 2.31$ s, $T_o + 4.61$ s.

The sudden opening of the gate initiated an initial phase dominated by a free-falling motion in the close proximity of the V-notch weir and the generation of a negative wave propagating

upstream into the reservoir. Only a limited volume of water was reached by the initial wave and the rest of the upstream tank water was still unaffected by the gate opening. The extent

Table 2

Digital appendix: movies of the unsteady V-notch thin plate weir experiments.

Filename	Original format	Deposited format	Description
IMGP0123.MPG	HD movie (1280 × 820 pixels) at 60 fps taken with Pentax K-01 and SMC Pentax-DA 40 mm f2.8 XS	MPEG-2 (25 fps)	Run 2. Sudden gate opening. Side view. Duration: 8 s.
IMGP0571.MPG	Movie (1280 × 720 pixels) at 30 fps taken with Pentax Optio WG-1	MPEG-2 (25 fps)	Run 5. Sudden gate opening. View from upstream. Duration: 12 s.

A**B****Fig. 4.** Photographs of the initial free-falling motion and its extent in the upstream reservoir ($t \times (g/h_0)^{1/2} < 2.23$), (A) side view (B) view from the reservoir.

of water volume affected by the free-falling motion was encompassed by a quasi-circular arc as illustrated in Fig. 4. In the close proximity of the weir, the free-surface shape appeared somehow similar to the inlet shape of a minimum energy loss (MEL) structure with its curved profile [2]. The resulting equipotential lines in a plan view highlighted the flow contraction under the action of gravity. The initial phase lasted less than 0.45 s: that is, for $t \times (g/h_0)^{1/2} < 2.23$ with $t=0$ at the start of gate opening.

The initial phase was followed by a dynamic phase during which the flow above the weir was close a quasi-steady overflow motion. The time-variations of the water elevation are illustrated in Fig. 5. The ensemble-averaged water elevation data were best fitted by:

$$\frac{h}{h_0} = \frac{12.72}{(t \times \sqrt{\frac{g}{h_0}} + 37.62)^{0.696}} \quad \text{for } 2.23 < t \times \sqrt{\frac{g}{h_0}} < 2400 \quad (2)$$

with a normalised correlation coefficient of 0.9999 for 76,621 data points. Eq. (2) was valid for the gradually-varied motion phase. During the initial instants ($t \times (g/h_0)^{1/2} < 2.23$), the time-variation of the water elevation exhibited a different shape as illustrated in Fig. 5B.

The rapid gate opening generated some disturbance in the water tank with the initial propagation of a three-dimensional negative

wave illustrated in Fig. 4. The reflections of the negative wave on the side walls and end walls of the tank yielded a complicated three-dimensional wave motion. During this gradually-varied phase, some seiche was observed in the tank. This is illustrated in Fig. 6 presenting the details of a typical water elevation signal. The seiche was associated with both longitudinal as well as transverse sloshing. The data highlighted some pseudo-periodic oscillations about a mean data trend (Fig. 6A). Some spectral analyses of the de-trended water elevation signals were performed using the method outlined by [14] and a typical data set is shown in Fig. 6B. In Fig. 6B, the two dominant frequencies are 0.830 and 1.074 Hz. The frequency analysis results are summarised in Fig. 7, where the dominant frequency data (dashed black lines) are compared with the first mode of natural sloshing in the longitudinal and transverse directions of the intake basin, respectively

$$F_L = \frac{2 \times L}{\sqrt{g \times (p+h)}} \quad (3a)$$

$$F_B = \frac{2 \times B}{\sqrt{g \times (p+h)}} \quad (3b)$$

where L is the tank length and B the tank width. Despite some data scatter, the findings were close to the theoretical calculations (Fig. 7).

4. Discussion

The instantaneous discharge Q through the V-notch weir was estimated using the integral form of the equation of conservation of mass for the water tank

$$\frac{d\text{Vol}}{dt} = -Q \quad (4)$$

where t is the time and Vol is the instantaneous volume of water in the intake structure

$$\text{Vol} = L \times B \times (h+p) \quad (5)$$

Eq. (5) assumed implicitly that the intake basin surface was horizontal and neglected the local drop in water elevation in the vicinity of the weir notch where the fluid was accelerated. The combination of Eqs. (4) and (5) gives an expression for the instantaneous overflow discharge

$$Q = -L \times B \times \frac{dh}{dt} \quad (6)$$

In the present study, Eq. (6) was calculated based upon the derivative of the smoothed water elevation data. The results are presented in Fig. 8. Overall the data were best correlated by

$$Q = C_d \times \frac{8}{15} \times \sqrt{2 \times g \times h^5} \quad (7a)$$

where Q is the water discharge, g the gravity acceleration and $C_d=0.58$ (Fig. 8). The result was close to earlier findings [13,16,9]. It may be rewritten in dimensionless form

$$\frac{Q}{\sqrt{g \times h_0 \times h_0^2}} = 0.58 \times \frac{8}{15} \times \sqrt{2 \times \left(\frac{h}{h_0}\right)^5} \quad (7b)$$

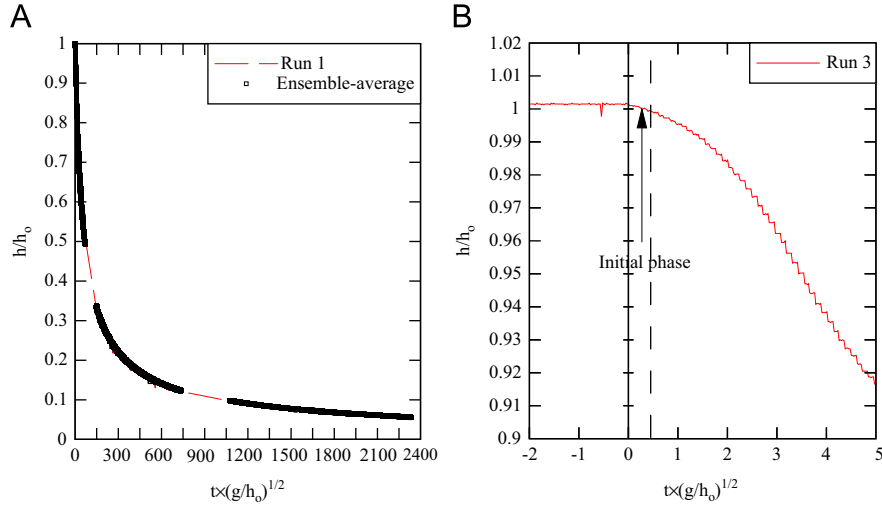


Fig. 5. Dimensionless time-variation of the upstream water elevation in the water tank, (A, left) comparison between a single data set and ensemble averaged data, (B, right) details of the initial phase during a single data set.

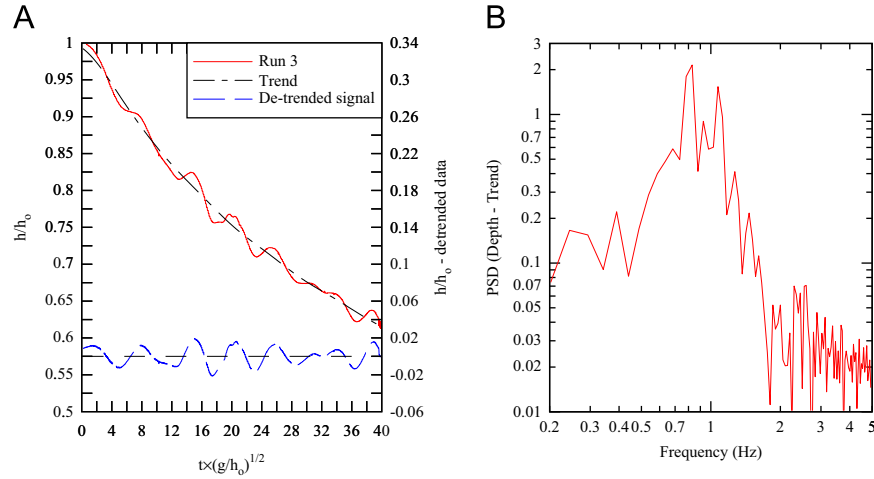


Fig. 6. Frequency analysis of the water elevation signal, (A) raw signal and de-trended water elevation signal, (B) power spectrum density function of the de-trended signal for $0 < t < 12$ s and $0.205 < h < 0.4$ m.

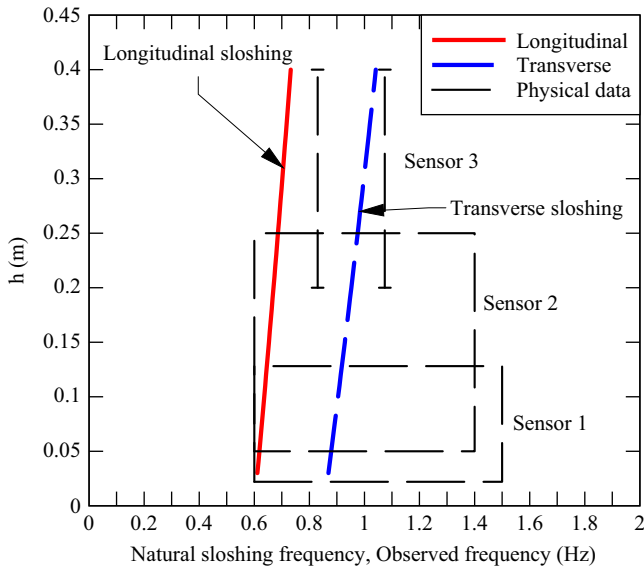


Fig. 7. Summary of frequency analyses of the free-surface elevation data—comparison between experimental observations (black dashed lines) and the first mode of natural sloshing frequency.

Basically the present findings showed that the unsteady discharge calibration of the V-notch weir yielded similar results to a more traditional calibration approach based upon steady flow experiments. A feature of the present unsteady method was the ability to test Eq. (7b) for a relatively wide range of discharges during each experimental run, without the need for a sustained steady flow rate.

The measurements herein were recorded for $0.022 < h < 0.40$ m. Although the results herein focused on water elevations within the range $0.025 < h < 0.40$ m, the Reynolds number $Q/(h \times \nu)$ became less than 1×10^4 for $h < 0.038$ m. It is conceivable that viscous scale effects might affect the findings for the smallest water elevations.

For completeness, during some unsteady experiments with a two-dimensional orifice flow, Chanson et al. [6] used the following discharge equation:

$$Q = C_d \times A \times \sqrt{2 \times g \times h} \quad (8)$$

where A is the orifice cross-section area and C_d was found to be $C_d \approx 0.58$. Assuming $A = h^2$ for a triangular V-notch weir, Eq. (8) becomes basically identical to Eq. (7a) despite the different geometries.

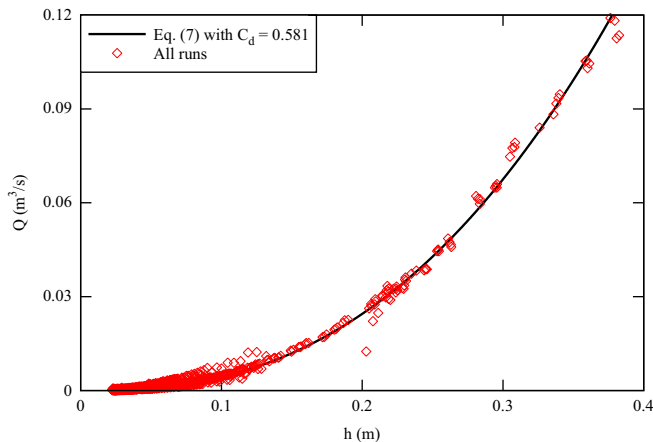


Fig. 8. Relationship between instantaneous discharge Q and upstream water depth h for the 90° V-notch weir—comparison between experimental data and Eq. (7a).

5. Conclusion

A discharge calibration of a large 90° V-notch thin plate weir was performed using an unsteady volume per time technique. The V-notch weir was initially closed by a fast-opening gate. The sudden opening induced an initial phase of the water motion followed by a gradually-varied flow phase. The initial phase was dominated by the free-falling motion of a volume of fluid in the vicinity of the weir and the generation of a negative wave propagating upstream into the reservoir. The water volume affected by the sudden opening was encompassed by a quasi-circular arc during the initial phase. During this gradually-varied phase, some seiche was observed in the tank. A frequency analysis of the water elevation data yielded results which compared favourably with the first mode of natural sloshing in the longitudinal and transverse directions of the intake basin, although the wave motion was three-dimensional.

The relationship between water discharge and upstream water elevation was derived from the integral form of the continuity equation based upon high-frequency water elevation recordings. The water elevation data were de-trended before processing. The results yielded a dimensionless discharge coefficient $C_d = 0.58$ close to previous findings for 90° V-notch weirs, as well as a series of unsteady orifice flow experiments. The findings showed that the unsteady discharge calibration of the V-notch weir yielded similar results to a more traditional calibration approach based upon steady flow experiments, enabling a relatively rapid calibration of the weir for a broad range of flow rates and upstream water levels. Another advantage is the ability to test relatively large flow rates, when the water supply (e.g. of a laboratory) cannot sustain such large steady flow rates.

Acknowledgements

The authors thank all the technical staff of the School of Civil Engineering (The University of Queensland) who assisted with the experiments. They acknowledge the helpful comments of Professor John Fenton (Tu Wien, Austria) and Dr. Oscar Castro-Orguaz (Institute of Sustainable Agriculture, Spanish National Research Council, IAS-CSIC, Spain). The financial support of the Australian Research Council (Grants DPDP0878922 and DP120100481) is acknowledged.

References

- [1] Ackers P, White WR, Perkins JA, Harrison AJM. Weirs and flumes for flow measurement. Chichester, UK: John Wiley; 1978 [327 pages].
- [2] Apelt CJ. Hydraulics of Minimum energy culverts and bridge waterways. Australian Civil Engineering Transactions. Institution of Engineers: Australia; 1983. vol. CE25, 2, p. 89–95.
- [3] Australian Standards. Measurement of water flow in open channels. Part 4: Measurement using flow gauging structures. Method 4.1: Thin-Plate Weirs. Australian Standard AS 3778.4.1–1991 (ISO 1438/1–1980), Council of Standards Australia; 1991 34 pages.
- [4] Bos MG. Discharge measurement structures. Publication no. 161. Delft Hydraulic Laboratory, Delft: The Netherlands; 1976. (Also Publication no. 20, ILRI, Wageningen, The Netherlands).
- [5] Bos MG, Replogle JA, Clemmens AJ. Flow measuring flumes for open channel systems. St. Joseph MI, USA: ASAE Publications; 1991 [321 pages].
- [6] Chanson H, Aoki S, Maruyama M. Unsteady two-dimensional orifice flow: a large-size experimental investigation. Journal of Hydraulic Research, IAHR 2002;40(1):63–71.
- [7] Chanson H, Wang H. Unsteady discharge calibration of a large V-notch weir. Hydraulic model report no. CH88/12. School of Civil Engineering, The University of Queensland. Brisbane: Australia; 2012. 50 pages & 4 movies (ISBN 9781742720579).
- [8] Darcy HPG, Bazin H. Recherches hydrauliques. (Hydraulic research). Imprimerie Impériales. Paris, France, Parties 1ère et 2ème (in French); 1865.
- [9] Herschy RW. General purpose flow measurement equations for flumes and thin plate weirs. Flow Measurement and Instrumentation 1995;6(4):283–293.
- [10] Herschy RW. Editorial to: open channel flow measurement. Flow Measurement and Instrumentation 2002;12:189–190.
- [11] International Organization for Standardization. Water flow measurement in open channels using weirs and venturi flumes—Part 1: Thin-plate weirs. ISO 1438/1–1980. International Organization for Standardization; 1980.
- [12] Lauber G. Experimente zur Talsperrenbruchwelle im glatten geneigten Rechteckkanal. (Dam break wave experiments in rectangular channels.) PhD thesis. VAW-ETH, Zürich: Switzerland; 1997 (in German). (also Mitteilungen der Versuchsanstalt für Wasserbau. Hydrologie und Glaziologie. ETH-Zürich, Switzerland, no. 152).
- [13] Lenz AT. Viscosity and surface tension effects on V-notch weir coefficients. Transactions of the American Society of Civil Engineers 1943;108(2195): 759–782 [Discussion: vol. 108, p. 783–802].
- [14] Press WH, Flannery BP, Teukolsky SA, Vetterling WT. Numerical recipes: the art of scientific computing. 3rd ed. Oxford, UK: Cambridge University Press; 2007 [1235 pages].
- [15] Soulis KX, Dercas N. Field calibration of weirs using partial volumetric flow measurements. Journal of Irrigation and Drainage Engineering, ASCE 2012;138(5):481–484. [http://dx.doi.org/10.1061/\(ASCE\)IR.1943-4774.0000424](http://dx.doi.org/10.1061/(ASCE)IR.1943-4774.0000424).
- [16] Trokolanski AT. Hydrometry: theory and practice of hydraulic measurements. Oxford, UK: Pergamon Press; 1960 [684 pages].